

LETTER TO THE EDITOR

The VLT-FLAMES Tarantula Survey. XV. VFTS 822: A candidate Herbig B[e] star at low metallicity \star , $\star\star$

V. M. Kalari^{1,2}, J. S. Vink¹, P. L. Dufton², C. J. Evans³, P. R. Dunstall², H. Sana⁴, J. S. Clark⁵, L. Ellerbroek⁶, A. de Koter^{6,7}, D. J. Lennon⁸, W. D. Taylor³

¹ Armagh Observatory, College Hill, Armagh, BT61 9DG, UK, e-mail: vek@arm.ac.uk

² Department of Physics & Astronomy, Queen's University Belfast, BT7 1NN, UK

³ UK Astronomy Technology Centre, Royal Observatory, Edinburgh, Blackford Hill, Edinburgh, EH9 3HJ, UK

⁴ ESA/STScI, 3700 San Martin Drive, Baltimore, MD 21218, USA

⁵ Department of Physics and Astronomy, The Open University, Walton Hall, Milton Keynes, MK7 6AA, UK

⁶ Astronomical Institute Anton Pannekoek, Amsterdam University, Science Park 904, 1098 XH, Amsterdam, The Netherlands

⁷ Instituut voor Sterrenkunde, KU Leuven, Celestijnenlaan 200D, 3001 Leuven, Belgium

⁸ European Space Astronomy Centre, Camino bajo del Castillo, Villanueva de la Cañada, E-28692 Madrid, Spain

Received 19 December 2013 / Accepted 13 January 2014

ABSTRACT

We report the discovery of the B[e] star VFTS 822 in the 30 Doradus star-forming region of the Large Magellanic Cloud, classified by optical spectroscopy from the VLT-FLAMES Tarantula Survey and complementary infrared photometry. VFTS 822 is a relatively low-luminosity ($\log L = 4.04 \pm 0.25 L_{\odot}$) B8[e] star. In this Letter, we evaluate the evolutionary status of VFTS 822 and discuss its candidacy as a Herbig B[e] star. If the object is indeed in the pre-main sequence phase, it would present an exciting opportunity to spectroscopically measure mass accretion rates at low metallicity, to probe the effect of metallicity on accretion rates.

Key words. Stars: emission-line, Be - Stars: pre-main sequence - Stars: supergiant - Stars: Hertzsprung-Russell diagram - Galaxies: Magellanic Clouds

1. Introduction

Present understanding suggests that most stars form by disc accretion during pre-main sequence (PMS) evolution. In the favoured accretion model, the disc forms during protostellar collapse and is disrupted by a stellar magnetosphere, which channels gas from the disc onto the stellar surface (see Hartmann 2008). Practical limitations have restricted observations of PMS stars to nearby solar-metallicity star-forming regions. Consequently, the properties of low-metallicity PMS stars, located in extra-galactic star-forming regions remain largely unknown.

The formation of stars may be significantly influenced by the metallicity (Z) of the local medium. The extra cooling provided by increasing Z is thought to decrease stellar mass. This is perhaps exemplified in the contrast between the present-day low-mass stellar initial mass function (IMF) and the anticipated high-mass population III IMF (Larson 1998). This may imply higher mass accretion rates at lower Z (Omukai & Palla 2001).

The only current possibility of observing low Z PMS stars spectroscopically is in the Magellanic clouds. Medium-resolution spectra, rather than photometric observations, are necessary as high-mass PMS systems at large distances become increasingly confused. They cannot be separated from more evolved systems occupying similar regions of the Hertzsprung-Russell (H-R) diagram using photometry alone. Another driver

for observing PMS stars spectroscopically is the possibility to measure mass accretion rates using different indicators.

Medium-resolution stellar spectroscopy with eight-to ten-metre class telescopes leads to a limiting magnitude of $V \sim 18$. In the nearest low- Z galaxy, the Large Magellanic Cloud (LMC) located at a distance of 50 kpc (Schaefer 2008), this translates to a mid-late B spectral type. These stars are more massive than $4 M_{\odot}$ and reside near the main sequence with a very short PMS phase. Therefore, detection of even a single PMS star is contentious, although several candidates have been reported (de Wit et al. 2005; Clayton et al. 2010; De Marchi et al. 2010).

One approach to identifying high-mass PMS stars is to discover them serendipitously from large spectroscopic surveys. The VLT-FLAMES Tarantula survey (VFTS; Evans et al. 2011) covering over 800 massive stars in the 30 Doradus starburst region of the LMC ($Z \sim 0.5 Z_{\odot}$) provides an ideal dataset for this task. From the VFTS sample, we identify VFTS 822 (RA(J2000) = $05^{\text{h}}39^{\text{m}}38.49^{\text{s}}$, Dec(J2000) = $-69^{\circ}09'00.5''$) as an accreting PMS candidate. We describe the characteristics of VFTS 822 that indicate it is in an accreting phase. However, since VFTS 822 exhibits the B[e] phenomenon (Lamers et al. 1998), its evolutionary status is unclear. Therefore, we explore the possibility that it could also be a B[e] supergiant.

2. Results

2.1. VFTS spectroscopy

Multi-epoch observations covering 3950 - 5050 Å ($R \approx 8000$) and 6450 - 6800 Å ($R = 16000$) were taken using the FLAMES

* Based on the observations at the European Southern Observatory Very Large Telescope in programme 182.D-0222.

** Table 1 and Figure 4 in on line version only.

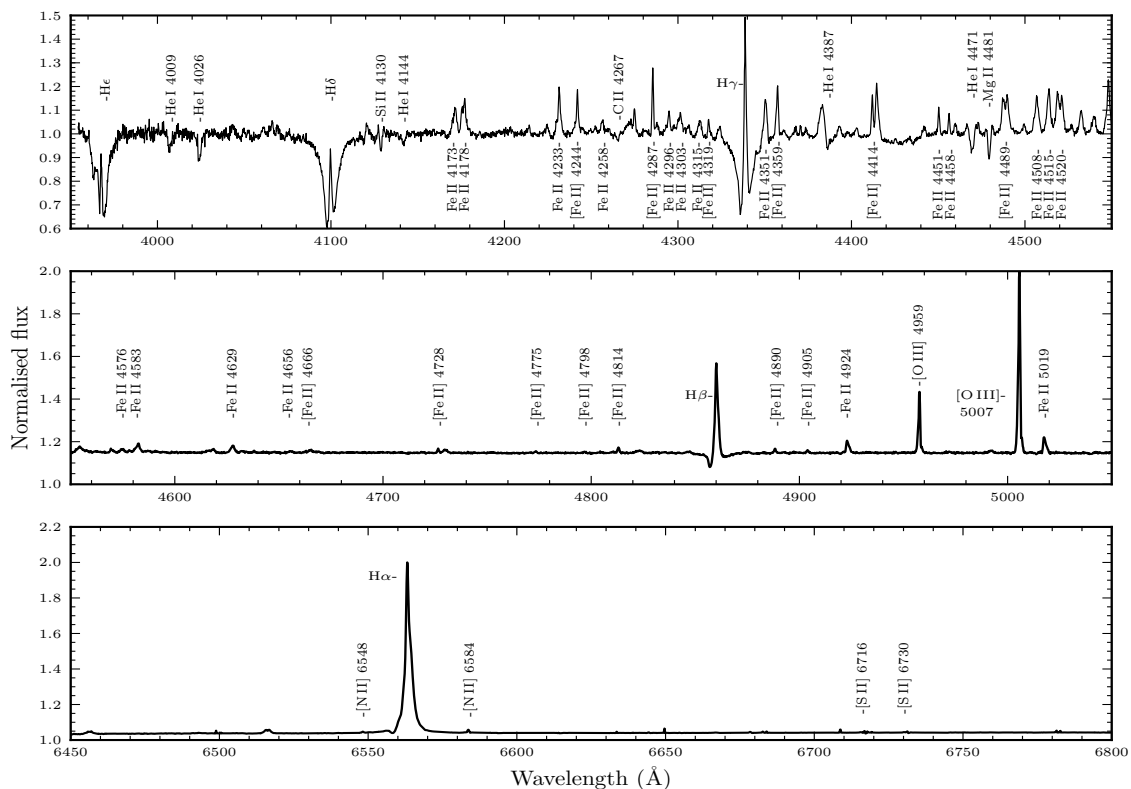


Fig. 1. Median FLAMES-Giraffe spectra of VFTS 822.

multi-fibre spectrograph (Pasquini et al. 2002). Further details on the observations and data reduction techniques can be found in Evans et al. (2011). Spectra of VFTS 822 are plotted in Fig. 1. Strong H α , H β , and H γ emission are seen, together with emission lines from both permitted and forbidden metal transitions. The intensity of the Si II λ 4128-30 and Mg II λ 4481 absorption, combined with the relative weakness of the He I lines at, e.g., λ 4009, 4026, argue for an approximate classification of B8 (particularly since we expect that the He I λ 4471 line is partly filled in by nebular contamination). Radial velocity (v_{rad}) estimates were obtained by profile fitting the He I lines at λ 4009, 4026 and 4143 and the Mg II λ 4481 doublet. A mean value of $262 \pm 7 \text{ km s}^{-1}$ was obtained. No evidence for binarity was found from peak-to-peak v_{rad} variations.

The estimation of atmospheric parameters is difficult because of the emission line spectrum that implies that a non-LTE photospheric model may not be appropriate. However, we have tried to provide constraints using the TLUSTY model atmospheres grid (Lanz & Hubeny 2007). The H δ and H γ profiles provide loci of estimates in the effective temperature and logarithmic gravity plane (T_{eff} , $\log g$). Possible solutions include (12000 K, 2.6) and (15000 K, 2.9). Assuming a normal helium abundance, the profile of the He I λ 4026 line is consistent with the former. The only well-observed metal line is the Mg II doublet, which leads to an upper magnesium abundance estimate (assuming zero microturbulence) of 6.87 dex for the lower T_{eff} . This is slightly smaller than found by Hunter et al. (2007) for the LMC using the same model atmosphere grid. As a result, T_{eff} is unlikely to be significantly lower than 12000 K. We adopt $T_{\text{eff}} = 12000 \pm 3000 \text{ K}$ and $\log g = 2.6 \pm 0.4$ as our best estimates. For spectra of this quality, the errors would normally be of the order of ($\pm 1000 \text{ K}$, ± 0.1), but the uncertainties in the appropriateness of the modelling implies that there might be additional uncertainties.

The H α equivalent width ($\text{EW}_{\text{H}\alpha}$) = $-67.5 \pm 4 \text{ \AA}$. The error reflects the difference obtained by fitting either the wings or the core. The $\text{EW}_{\text{H}\alpha}$ is greater than maximum measured values for classical Be stars of $\gtrsim -50 \text{ \AA}$ (Jones et al. 2011). The H β equivalent width ($\text{EW}_{\text{H}\beta}$) = $-2.72 \pm 0.5 \text{ \AA}$.

2.2. Photometry

Broad-band photometry for VFTS 822 was adopted from the published catalogues summarised in Table 1. The broadband photometry was not used to estimate extinction, because the emission line contribution to the continuum, although small, cannot be well constrained. We therefore employed equivalent width measurements of the λ 4428 and λ 6614 diffuse interstellar band features. From van Loon et al. (2013), $A_V = \text{EW}_{4428}/0.7$ and $A_V = \text{EW}_{6614}/0.03$. This leads to an estimated extinction of $A_V = 1.75 \pm 0.05$ (where the observed scatter is not accounted for).

Using an ATLAS9 model (Castelli & Kurucz 2004) having $T_{\text{eff}} = 12000 \text{ K}$, $\log g = 2.6$, $[\text{M}/\text{H}] = -0.5$, we calculated a bolometric correction, $\text{BC} = -0.673$. We estimate the logarithm of the luminosity, $\log L = 4.04 \pm 0.25 L_{\odot}$. The error accounts for the variation in BC due to the uncertainty in T_{eff} . This is most likely an upper limit, since the disc contribution is considered negligible. The luminosity is greater than expected for a mid-late B-type star, but not unprecedented for Herbig stars. For example, HD 85567, V594 Cas, and V921 Sco each have $\log L \gtrsim 4 L_{\odot}$ and are all classified as Herbig B[e] stars (Lamers et al. 1998; Kraus et al 2012).

2.3. Infrared properties

The SED slope (α) in the infrared is an essential tool for diagnosing the nature of any infrared excess. We follow Lada et

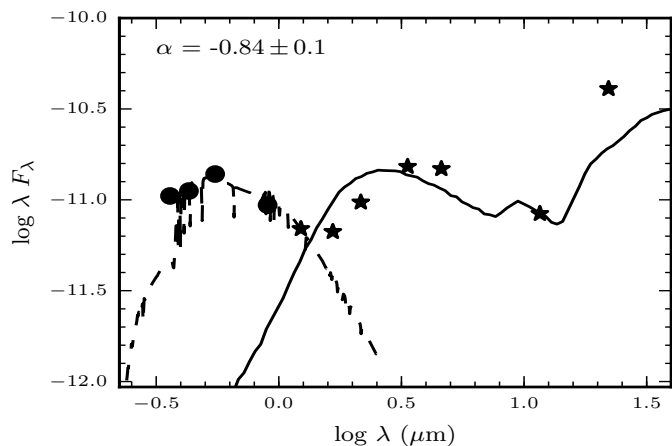


Fig. 2. Observed fluxes in optical (circles) and IR (asterisks). The dashed line is the model SED and the solid line the best-fit YSO model. al. (1987), where $\alpha = d \log(\lambda F_\lambda) / d \log \lambda$ and $\lambda > 3 \mu\text{m}$. WISE photometry was not used to calculate α because it is possibly affected by nebulosity at $\lambda > 10 \mu\text{m}$. We therefore calculated α based on *Spitzer* photometry alone. For VFTS 822, $\alpha = -0.84 \pm 0.1$, which is greater than $\alpha \sim -3$, as expected for normal OB stars (Sung et al. 2009). It is a Class II PMS object based on the scheme devised by Lada et al. (1987). The SED slope closely resembles the one for objects with a dusty disc, $\lambda F_\lambda \propto \lambda^{-2/3}$, i.e., a much slower decrease with wavelength than for most evolved stars.

A diagnostic feature of dusty discs is $(K - 24 \mu\text{m}) \geq 5$ (e.g. Hernandez et al. 2006). For VFTS 822, $K_s - 22 \mu\text{m} \sim 9$ mag, indicating the likely presence of a dusty disc. In Fig. 2, we plot the optical-infrared SED for VFTS 822. Overplotted is the extinction corrected adopted ATLAS9 model spectrum. The solid line is the best-fit young stellar object (YSO) model ($\chi^2 = 85$) from Robitaille et al. (2007). The SED slope and infrared colours indicate that VFTS 822 has a dusty circumstellar disc characterised by a disc temperature of ~ 950 K.

3. Evolutionary status

In low-mass stars, emission line spectra and dust discs are unique to the PMS phase. However, at Herbig Be masses, B[e]-type stars also display similar characteristics. B[e]-type stars are rare and heterogeneous in terms of their evolutionary status. They include both PMS objects and evolved supergiants (sg). Based on the spectral type, emission line features, and infrared properties, we consider VFTS 822 to be a B[e]-type star (see Lamers et al. 1998). Identifying the evolutionary status of VFTS 822 is challenging because the observed properties of sgB[e]-type stars and PMS Herbig-B[e] stars that have $L \sim 4\text{--}4.5 L_\odot$ are similar. Therefore, in the following sections we discuss the possibility that VFTS 822 might be either a PMS B[e] star or an sgB[e] star.

3.1. B[e] supergiant?

The best fit $\log g$ (2.6 ± 0.4) is larger than the values measured for many late B-type sg (cf. Firnstein & Przybilla 2012, where $\log g \sim 2$ is typical). Owing to the emission lines spectra, abundances are challenging to determine, but we do not see the compelling evidence of chemical evolution that we might expect for an sgB[e] star (e.g. no N II $\lambda\lambda 3995, 4630$ features are seen). However, the lack of evidence for He enrichment suggests that nitrogen enrichment need not necessarily be present. Therefore,

one cannot exclude the possibility that VFTS 822 is a supergiant. One promising avenue forward would be to compare the enrichment of CO¹³ to CO¹² infrared bands (Kraus et al. 2009).

If VFTS 822 is an sgB[e] star, it has an age of 36 Myr, with a lower error bar of 4 Myr based on the single star isochrones of Marigo et al. (2008). This is significantly older than the estimated age of R136, the central cluster of 30 Dor (1-2 Myr), and the high-mass population in the surrounding nebula (e.g. Walborn & Blades, 1997). The v_{rad} of VFTS 822 is similar to other stars in the region (Sana et al. 2013), making it unlikely to be an interloper. Nonetheless, the possibility of a genuine 36 Myr old sgB[e] cannot be ruled out because of the complex star-formation scenario and age spread present within 30 Dor. However, the inherent rarity of sgB[e] stars means that a large initial population is expected to yield them (Clark et al. 2013). Such a population, which should be readily identifiable via the resulting IR bright red supergiant/super-AGB cohort, is not known to be present within the immediate vicinity (Bonanos et al. 2009).

3.2. Or Herbig B[e] star?

The position of VFTS 822 in the H-R diagram is compared to known LMC sgB[e] (Zickgraf 2006) and Galactic Herbig B[e] stars (Lamers et al. 1998) in Fig. 3. No Herbig B[e] stars have been discovered yet in the LMC. Birthlines with mass accretion rates (\dot{M}_{acc}) of 10^{-4} and $10^{-3} M_\odot \text{yr}^{-1}$ from Hosokawa & Omukai (2009) are plotted, along with the zero-age main sequence from Schaerer et al. (1992) and $10^{4.5}$ yr PMS isochrone from Bressan et al. (2012). The position of VFTS 822 on the H-R diagram is coincident with a low-luminosity LMC sgB[e], but it sits in an H-R diagram position that is also covered by known Galactic Herbig B[e] stars. The comparable positions of sgB[e] and Herbig stars at $\log L < 4.5 L_\odot$ make establishing the evolutionary status of VFTS 822 non-trivial.

If VFTS 822 is a PMS, it has a \dot{M}_{acc} of $3 \pm 1 \times 10^{-4} M_\odot \text{yr}^{-1}$, a mass (M_*) of $10.7 \pm 1 M_\odot$, and age ≈ 30000 yrs according to the PMS models. PMS stars at such masses have extremely short PMS lifetimes, but a few have been detected (Drew et al. 1997). VFTS 822 is expected to be past its protostellar phase and to be accreting mass. At this age and mass, the \dot{M}_{acc} of the object is expected to be relatively high, as is necessary to overcome the radiative pressure. Hosokawa & Omukai (2009) predict that at high \dot{M}_{acc} ($> 10^{-4} M_\odot \text{yr}^{-1}$), massive stars ($> 10 M_\odot$) are seen in the PMS phase. We find that the theoretically predicted \dot{M}_{acc} are similar to the observed accretion rates calculated in Sec. 3.2.1.

The estimated $\log g$ of VFTS 822 (2.6 ± 0.4) is somewhat lower than expected for PMS stars. However profile fitting of Herbig stars for $\log g$ determination is not common practice, with a recent result showing a Galactic Herbig star to have a $\log g$ value of 3.5, similar to giant stars (Ochsendorf et al. 2011). Given the modest extinction toward VFTS 822, this implies a relatively large stellar radius of over $10 R_\odot$. This may, however, be symptomatic of a bloated star, where very high \dot{M}_{acc} causes stars to bloat

VFTS 822 is located near the edge of the 30 Dor nebula at $5.8'$ from R136 (approx. 84.4 pc at the distance to the LMC) as shown in Fig. 4. This region contains previously identified loosely grouped Class II PMS objects, which includes the *Spitzer* counterpart of VFTS 822 (Kim et al. 2007), whereas YSOs or Class I objects are situated nearer to R136. It is located on the edge of filamentary structure, where one might expect to find Class II PMS objects (Hartmann 2008).

3.2.1. \dot{M}_{acc}

Balmer line emission, especially $H\alpha$, is a commonly used accretion tracer. It is thought to originate in the magnetospheric accretion columns (Calvet & Hartmann 1992). The line luminosity (L_{line}) can be used to measure the \dot{M}_{acc} . To calculate L_{line} from $H\alpha$ and $H\beta$, we assume that the excess flux in the continuum is negligible. This assumption is correct if there is no significant veiling. Since photospheric absorption lines are visible, we assume this is justified. The line flux (F_{line}) is given by

$$F_{\text{line}} = F_{\text{cont}} \times \text{EW}_{\text{line}}. \quad (1)$$

Here F_{cont} is the continuum flux. The continuum flux was measured using the adopted ATLAS9 model spectra. The average flux of the model over the 6556 - 6570 Å and 4856 - 4864 Å ranges was taken as the $H\alpha$ and $H\beta$ continuum flux, respectively. Multiplying by $4\pi d^2$, we obtain the respective L_{line} . Based on the accretion luminosity (L_{acc})- L_{line} relation of Herczeg & Hillenbrand (2008), we determine $\log L_{\text{acc}} = 3.89 \pm 0.6 L_{\odot}$ from $H\alpha$ and $\log L_{\text{acc}} = 3.58 \pm 0.6 L_{\odot}$ from $H\beta$. The errors include the RMS scatter in the L_{acc} - L_{line} relations.

Another commonly used accretion indicator is the Balmer jump. The excess luminosity is thought to be caused by an accretion shock on the stellar surface. The UV excess of VFTS 822, $(U-I) - (U-I)_0 = -0.742$, can be used to measure its accretion rate. The observed $(U-I)$ colour was corrected for extinction, and the $(U-I)_0$ model colour was determined using the model spectrum and appropriate filter responses. The excess U-band luminosity, $\log L_{(U, \text{excess})} = 2.96 \pm 0.3 L_{\odot}$, and the accretion luminosity $L_{\text{acc}} = 3.96 \pm 0.5 L_{\odot}$. The \dot{M}_{acc} is given by the free-fall equation. Following the assumptions of Herczeg & Hillenbrand (2008),

$$\log \dot{M}_{\text{acc}} = -7.39 + \log L_{\text{acc}}/L_{\odot} + \log R_*/R_{\odot} - \log M_*/M_{\odot}. \quad (2)$$

Here \dot{M}_{acc} is in units of $M_{\odot} \text{yr}^{-1}$. We calculate a median \dot{M}_{acc} of $3.16 \pm 2 \times 10^{-4} M_{\odot} \text{yr}^{-1}$ from the three indicators. The L_{acc} - L_{line} , L_{acc} - $L_{U, \text{excess}}$ relations adopted are tested well on Z_{\odot} PMS stars, up to Herbig Ae masses ($\lesssim 4 M_{\odot}$). We therefore acknowledge that they may not be numerically applicable to VFTS 822, but only provide an order-of-magnitude estimate. The applied magnetospheric accretion model has been considered valid for spectral types up to late B, but not for the majority of Herbig Be stars (Mottram et al. 2007; Monnier et al. 2005).

The agreement between the \dot{M}_{acc} calculated from the $H\alpha$, $H\beta$, U -band luminosities suggests that the Balmer lines and jump are produced in the same mass accretion phenomenon, favouring a PMS evolutionary phase.

4. Conclusions

VFTS 822 is a B8 star with estimated parameters of $T_{\text{eff}} = 12000 \pm 3000$ K, $\log g = 2.6 \pm 0.4$, and $\log L = 4.04 \pm 0.25 L_{\odot}$. Both $H\alpha$ and $H\beta$ are in emission, along with forbidden and permitted metal lines. A UV and infrared excess is found when compared to model colours. It is considered to exhibit the B[e] phenomenon. Therefore, its location in the H-R diagram does not clarify its evolutionary status. Thus, we suggest that:

- (i) VFTS 822 may be an sgB[e] star, around 35 Myr, which we consider quite unlikely (see Sec. 3.1).
- (ii) Alternatively, VFTS 822 could be a Herbig B[e] PMS star with an age of ≈ 30000 years, a mass of $10 M_{\odot}$, and a $\dot{M}_{\text{acc}} \sim 10^{-4} M_{\odot} \text{yr}^{-1}$.

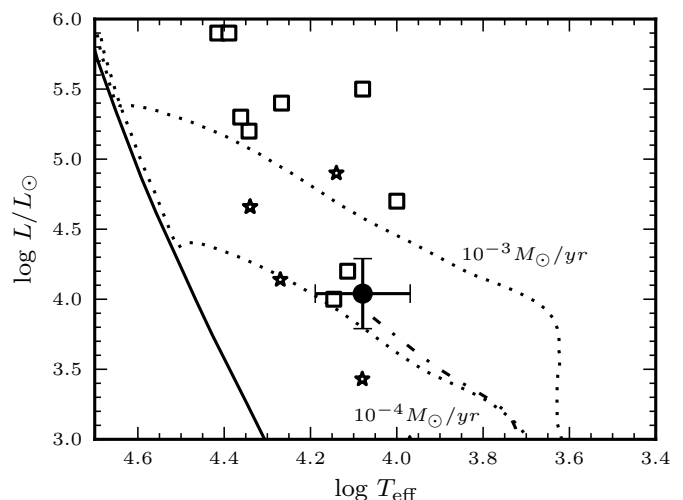


Fig. 3. H-R diagram showing the position of VFTS 822 (circle), LMC sgB[e] (squares), Galactic PMS B[e] (asterisks), model birthlines (dotted lines), MS (solid line), and PMS (dashed-dotted line) isochrones.

The lack of evolutionary abundance enrichment and a UV excess favour a PMS rather than post main sequence star. The low $\log g$ may be explained as the result of a bloated radius due to the large \dot{M}_{acc} . Because no similar PMS stars have been discovered, comparing properties is not feasible at this point. At the measured and predicted \dot{M}_{acc} , VFTS 822 is expected to have a short PMS lifetime. While the probability of observing a true PMS star in this very small gap of time is serendipitous, our observations suggest that VFTS 822 is a genuine PMS candidate.

We conclude that if VFTS 822 is a PMS B[e] star, it is a rare object and worthy of future study. Further data is required to clarify its evolutionary status.

References

- Bonanos, A. Z., Massa, D. L., Sewilo, M., et al. 2009, *AJ*, 138, 1003
Bressan, A., Marigo, P., Girardi, L., et al. 2012, *MNRAS*, 427, 127
Calvet, N., & Hartmann, L. 1992, *ApJ*, 386, 239
Castelli, F., & Kurucz, R. L. 2004, arXiv:astro-ph/0405087
Clark, J. S., Ritchie, B. W., & Negueruela, I. 2013, *A&A*, 560, A11
Clayton, G. C., Sargent, B., Boyer, M. L., et al. 2010, *ApJ*, 722, 1131
Cutri, R. M., & et al. 2012, *VizieR Online Data Catalog*, 2311, 0
Cutri, R. M., & et al. 2003, *VizieR Online Data Catalog*, 2246, 0
De Marchi, G., Panagia, N., & Romaniello, M. 2010, *ApJ*, 715, 1
de Wit, W.J., Beaulieu, J.P., Lamers, H.J.G.L.M., & et al. 2005, *A&A*, 432, 619
Drew, J. E., Busfield, G., Hoare, M. G., et al. 1997, *MNRAS*, 286, 538
Evans, C. J., Taylor, W. D., Hénault-Brunet, V., et al. 2011, *A&A*, 530, A108
Firnstein, M., & Przybilla, N. 2012, *A&A*, 543, A80
Hartmann, L. 2008, *Accretion Processes in Star Formation*, CUP, 2008,
Herczeg, G. J., & Hillenbrand, L. A. 2008, *ApJ*, 681, 594
Hernández, J., Briceño, C., Calvet, N., et al. 2006, *ApJ*, 652, 472
Hosokawa, T., & Omukai, K. 2009, *ApJ*, 691, 823
Hunter, I., Dufton, P. L., Smartt, S. J., et al. 2007, *A&A*, 466, 277
Jones, C. E., Tycner, C., & Smith, A. D. 2011, *AJ*, 141, 150
Kim, H.-S., Kim, S., Bak, J.-Y., et al. 2007, *ApJ*, 669, 1003
Kraus, S., Calvet, N., Hartmann, L., et al. 2012, *ApJ*, 752, 11
Kraus, M. 2009, *A&A*, 494, 253
Lada, C. J. 1987, *Star Forming Regions*, 115, 1
Lamers, H.J.G.L.M., Zickgraf, F.J., de Winter, D., & et al. 1998, *A&A*, 340, 117
Lanz, T., & Hubeny, I. 2007, *ApJS*, 169, 83
Larson, R. B. 1998, *MNRAS*, 301, 569
Marigo, P., Girardi, L., Bressan, A., et al. 2008, *A&A*, 482, 883
Meixner, M., Gordon, K. D., Indebetouw, R., et al. 2006, *AJ*, 132, 2268
Monnier, J. D., Millan-Gabet, R., Billmeier, R., et al. 2005, *ApJ*, 624, 832
Mottram, J. C., Vink, J. S., Oudmaijer, R. D., & Patel, M. 2007, *MNRAS*, 377, 1363
Ochsendorf, B. B., Ellerbroek, L. E., Chini, R., et al. 2011, *A&A*, 536, L1
Omukai, K., & Palla, F. 2001, *ApJ*, 561, L55
Pasquini, L., Avila, G., Blecha, A., et al. 2002, *The Messenger*, 110, 1
Robitaille, T.P., Whitney, B.A., Indebetouw, R., & Wood, K. 2007, *ApJS*, 169, 328
Sana, H., de Koter, A., de Mink, S. E., et al. 2013, *A&A*, 550, A107
Schaerer, D., Meynet, G., Maeder, A., & Schaller, G. 1993, *A&AS*, 98, 523
Schaefer, B. E. 2008, *AJ*, 135, 112
van Loon, J. T., Bailey, M., Tatton, B. L., et al. 2013, *A&A*, 550, A108
Walborn, N. R., & Blades, J. C. 1997, *ApJS*, 112, 457
Zaritsky, D., Harris, J., Thompson, I. B., & Grebel, E. K. 2004, *AJ*, 128, 1606
Zickgraf, F.-J. 2006, *Stars with the B[e] Phenomenon*, 355, 135

Table 1. Adopted photometry for VFTS 822

| Band | Magnitude | Ref. | Band | Magnitude | Ref. |
|-----------|-------------------|------|--------------------|-------------------|------|
| <i>U</i> | 15.395 ± 0.03 | 1 | $3.3 \mu\text{m}$ | 10.648 ± 0.02 | 3 |
| <i>B</i> | 16.028 ± 0.31 | 1 | $3.6 \mu\text{m}$ | 10.402 ± 0.02 | 4 |
| <i>V</i> | 15.433 ± 0.02 | 1 | $4.5 \mu\text{m}$ | 9.775 ± 0.02 | 4 |
| <i>I</i> | 14.926 ± 0.02 | 1 | $4.6 \mu\text{m}$ | 9.696 ± 0.02 | 3 |
| <i>J</i> | 14.246 ± 0.03 | 2 | $5.8 \mu\text{m}$ | 8.206 ± 0.02 | 4 |
| <i>H</i> | 13.557 ± 0.02 | 2 | $8.0 \mu\text{m}$ | 8.662 ± 0.02 | 4 |
| <i>Ks</i> | 12.296 ± 0.02 | 2 | $11.6 \mu\text{m}$ | 7.383 ± 0.02 | 3 |
| | | | $22.1 \mu\text{m}$ | 3.606 ± 0.04 | 3 |

References. (1) Zaritsky et al. (2004); (2) Cutri et al. (2003); (3) Cutri et al. (2012); (4) Meixner et al. (2006)

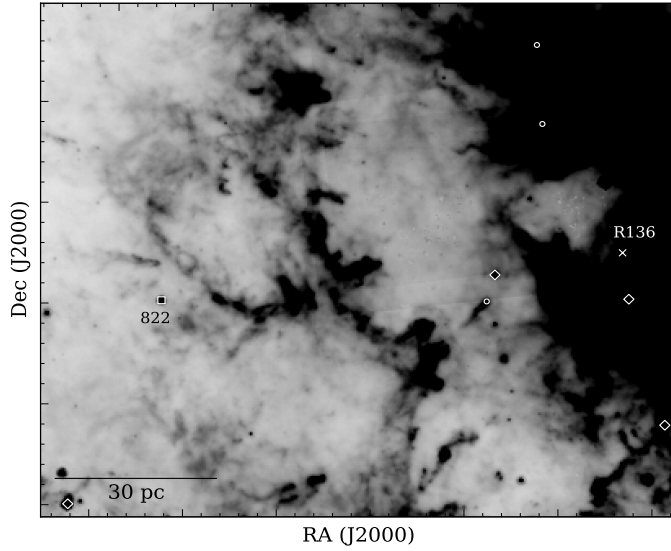


Fig. 4. Spitzer $8 \mu\text{m}$ image showing the position of VFTS 822 (square) with respect to R136 (cross). North is up and east is to the left. Circles and diamonds are known Class I and Class II sources, respectively.